Intensification of UV-C treatment to remove emerging contaminants by UV-C/H2O2 and UV-C/S2O82–: Susceptibility to photolysis and investigation of acute toxicity

Maria Clara V.M. Starling, Patterson Souza, Annaïg Le Person, Camila Amorim, Justine Criquet

INTENSIFICATION OF UV-C TREATMENT TO REMOVE EMERGING CONTAMINANTS BY UV-C/H_2O_2 AND UV-C/$S_2O_8^{2-}$: SUSCEPTIBILITY TO PHOTOLYSIS AND INVESTIGATON OF ACUTE TOXICITY

Maria Clara V.M. Starling[1,2], Patterson P. Souza[3], Annaïg Le Person[2], Camila C. Amorim[1*], Justine Criquet[2]

(1) Universidade Federal de Minas Gerais, Research Group on Environmental Applications of Advanced Oxidation Processes, 31270-901, Belo Horizonte, Brazil

(2) Université de Lille CNRS, UMR 8516 – LASIR, Equipe Physico-Chimie de l'Environnement F-59000 Lille, France

(3) Centro Federal de Educação Tecnológica de Minas Gerais, Chemistry Department, 30421-169, Belo Horizonte, MG, Brazil

*Corresponding author: camila@desa.ufmg.br. Universidade Federal de Minas Gerais, Av. Presidente Antônio Carlos 6627, 31270-901, Belo Horizonte, Brazil. Telephone: +55 31 3409-3677, Fax: +55 31 4409-1879.

GRAPHICAL ABSTRACT

ABSTRACT

In this study, the degradation of four emerging contaminants (losartan potassium (LP), furosemide (FRSM), caffeine (CAF), and carbendazim (CBZ) under UV-C, UV-C/H_2O_2, and UV-C/$S_2O_8^{2-}$ was investigated. A comparative evaluation of the efficiency of UV-C/H_2O_2 and UV-C/$S_2O_8^{2-}$ in the degradation of these target CECs has not yet been reported. Moreover, target compounds were submitted to UV-C/AOPs individually in pure water and their simultaneous degradation was investigated in real surface water. Evolution of the acute toxicity of each compound during treatment was evaluated using *Alivibrio fischeri.* Quantum yields were determined for LP (0.011 to 0.016), FRSM (0.024 to 0.092), CAF (0.0007 to 0.0009), and CBZ (0.0016 to 0.0036) at different pH values. UV-C/H_2O_2 and UV-C/$S_2O_8^2$ achieved more than 98% removal of all compounds within 600 mJ cm^{-2}, and pseudo-fist-order kinetic constants (k'_{app}) for the

degradation reactions were up to seven times higher in the presence of these oxidants when compared to *k'$_{app}$ values obtained for UV-C photolysis*. k'$_{app}$ measured for UV-C/H_2O_2 were higher than those calculated for UV-C/$S_2O_8^{2-}$ except in the case of LP. Acute toxicity analysis suggested the formation of toxic intermediates during the UV-C photolysis of LP and FRSM, and the degradation of LP via UV-C/$S_2O_8^{2-}$ also enhaced acute toxicity although electric energy efficiency per order identified UV-C/$S_2O_8^{2}$ as the most efficient process for the removal of this compound. Finally, different transformation products obtained during the degradation of caffeine under the different UV-C AOPs suggested that distinct degradation routes were involved in each treatment tested.

Keywords: advanced oxidation processes, persulfate, UV-C process, quantum yield, contaminants of emerging concern

1. Introduction

After the scientific community raised awareness regarding the presence of contaminants of emerging concern (CECs) in different water resources (i.e. drinking water, groundwater, surface water, and wastewater) these compounds have been intensively studied over the past two decades. Therefore, many technologies have been developed for the removal of CECs from these matrices.

Advanced oxidation processes (AOPs) have proven to be effective methods for the degradation of CECs [1]. AOPs incorporating UV-C irradiation (UV-C AOPs) are attractive alternatives within this category [2, 3], because the UV-C reactors already being used worldwide in water and wastewater treatment plants could be easily adapted for these processes [4].

Photoperoxidation (UV-C/H_2O_2) is one of the most disseminated AOPs [5], wherein H_2O_2 undergoes UV-C photolysis (λ=254 nm) and is cleaved into two hydroxyl radicals (HO•) [6]. HO• presents a high redox potential (E^0= 1.8–2.7 V), thus being highly reactive and non-selective [7]. In addition, the UV-C/H_2O_2 process does not require pH adjustment, simplifying operational requirements in comparison to those involved in other AOPs such as Fenton and photo-Fenton [8, 9].

Most of the studies using UV-C/H_2O_2 to remove CECs from water have used pure solutions of target compounds in synthetic matrices [6, 10-12]. Meanwhile, in real matrices containing natural organic matter (NOM), inorganic ions (HCO_3, Cl^-, NO_3^-, and SO_4^{2-}), and dissolved oxygen (DO), UV-C/H_2O_2 reactions may be disturbed due to quenching of HO• [13], thus reducing the process efficiency. There has,

thus, been increased interest in alternative systems that employ strongly reactive yet selective radicals, such as the sulfate radical (SO_4^{-}•) [14].

In irradiated systems, SO_4^{-}• (E^0 = 2.55–3.1 V) is formed when persulfate (PS, $S_2O_8^{2-}$) or peroxymonosulfate (PMS, SO_5^{2-}) are cleaved under UV-C (254 nm) irradiation [15]. SO_4^{-}• reacts primarily via an electron transfer mechanism, and is, thus, more selective and resistant than HO• in the presence of matrix constituents such as NOM and inorganic ions [16]. In addition, SO_4^{-}• is not as easily influenced by carbonate ions (HCO_3^{-}) due to the lower rate constant of the reaction between SO_4^{-}• and HCO_3^{-} (2.6 to 9.1 x 10^6 M^{-1} s^{-1}) compared to that of the reaction between HO• and HCO_3^{-} (10^7 M^{-1} s^{-1}) [6, 14, 17-20]. The removal of CECs via UV-C/H_2O_2 and UV-C/$S_2O_8^{2-}$ varies according to the chemical structure of the compound involved and as a consequence of the different reaction mechanisms promoted by each radical [2, 21, 22].

Toxic intermediates may be generated during UV-C AOPs [23], and appropriate treatment conditions for the simple removal of target compounds may not effectively eliminate their toxic effects [24]. Therefore, it is essential to follow the evolution of the toxicity of compounds during their treatment by UV-C AOPs in order to comprehensively understand treatment efficiency [25], especially with regard to UV-C/$S_2O_8^{2-}$, for which only a few studies have investigated toxicity evolution [26, 27]. In addition, since in industrial applications these advanced treatments would not be utilized to achieve complete mineralization of CECs, it is necessary to investigate the evolution of toxicity resulting from the degradation of various harmful CECs present in environmental samples, as well as to identify any intermediates and/or byproducts of their degradation processes.

Considering the vast diversity of emerging contaminants present in surface water, four CECs were chosen as representative compounds for different classes of contaminants because of their environmental relevance as they have been increasingly consumed and consequently detected in surface water worldwide. Losartan potassium (LP) and furosemide (FRSM) represent pharmaceutical drugs. These compounds are widely prescribed to hypertensive patients worldwide and have been detected in environmental matrices in various locations [28-33], especially in developing countries where sanitary conditions are inadequate [34]. Caffeine (CAF) was chosen due to its regular occurrence in surface water and drinking water resources, for which it was recently proposed as an urban pollution tracer [35-37]. The fungicide carbendazim (CBZ), which has been detected in surface water around the world and is known for its toxicity, represents the diverse group of agrochemicals [36, 38, 39].

In this context, the goals of this study were to assess the susceptibility LP, FRSM, CAF and CBZ to UV-C photolysis; to evaluate the performance of UV-C/$S_2O_8^{2-}$ and UV-C/H_2O_2 in the degradation of each target compound individually in pure water as well as that of the four compounds in conjunction in pure water and real surface water; and to investigate the impact of each UV-C AOP on acute toxicity.

2. Material and Methods

2.1 Determination of quantum yields

LP, FRSM, CAF, and CBZ were purchased from Sigma-Aldrich. Table S1 (Supplementary Material) shows the chemical structures and some physicochemical properties of each of the four CECs. Figure S1 shows the UV-Vis absorption spectra of the CECs at the natural pH of each solution.

Experiments for the determination of quantum yields (Φ) were conducted in a UV-C bench reactor (volume 0.0035 L, pathway length 1 cm^{-2}) equipped with a low-pressure mercury-xenon lamp (LightningCure LC8, Hamamatsu City, Japan) under constant agitation by using a magnetic stirrer. Lamp intensity (I_0) was determined prior to experiments using H_2O_2 (I_0 = 2.54 J m^{-2} s^{-1}) and atrazine (I_0 = 2.14 J m^{-2} s^{-1}) as actinometers [40, 41]. A UV filter (254 nm; Semrock MaxLamp) was placed at the light source. Initial concentrations of LP, FRSM, CAF, and CBZ were 2.2, 3.0, 5.2, and 5.5 µM, respectively. Quantum yields were calculated by quantifying the decay of each compound when exposed to light at pH = 3.0, the natural pH of the solution (6.0 for LP, 5.5 for FRSM, 5.8 for CAF, and 7.1 for CBZ), and at pH = 9. The pH was adjusted using 0.01 M HCl or 0.01 M NaOH solutions.

The photolysis coefficient (C_p) was calculated for each of the target compounds. C_p is defined as the product of the quantum yield (Φ_{254nm}) and the molar attenuation coefficient (ε_{254nm}) of a substance, and can be calculated according to Equations 1 and 2 [4]:

$$k_d = (\Phi_{254nm} \times \varepsilon_{254nm} \times 2302)/U = (Cp \times 2302/U) \quad \text{(Eq. 1)}$$

$$Cp = (k_d \times U)/2302 \quad \text{(Eq. 2)}$$

where k_d is the fluence-based pseudo-first-order rate constant (units J^{-1} cm^{-2}), U is the energy per mole of photons at 254 nm (4.72 x 10^5 J $Einstein^{-1}$), and 2302 is a factor used for unit conversion purposes (base 10 to base e, and mJ to J).

2.2 High-Performance Liquid Chromatography analyses

A liquid chromatograph equipped with a UV detector (Agilent 1260 Infinity II

series, UV and diode array detector equipped with a 60 mm high-sensitivity cell) was used for the quantification of CECs. The separation was performed on C_{18} columns (Poroshell 120 EC-C18 (3 x 50 mm, internal diameter 2.7 µm) followed by Poroshell HPH-C18 (4.6 x 150 mm, internal diameter 2.7 µm) at a flow rate of 0.5 mL min^{-1}. Ultra-pure water (40%) and MeOH (60%; MERCK HPLC grade, 98% purity), both containing 0.1% formic acid (SIGMA-ALDRICH HPLC grade, 98% purity), was used as the mobile phase for LP and FRSM, adapting previously described procedures [42]. Both LP and FRSM were monitored at λ=240 nm. Methods adapted from those described by the USA Environmental Protection Agency (EPA) [43, 44] were used for the quantification of CAF (MeOH/H_2O 30/70 (v/v), 273 nm) and CBZ (MeOH/H_2O 50/50 (v/v); 285 nm).

2.3 Degradation of target compounds by UV-C AOP

UV-C, UV-C/H_2O_2, and UV-C/$S_2O_8^{2-}$ treatments were performed in a 2 L cylindrical bench photo-reactor equipped with a low-pressure mercury vapor lamp emitting monochromatic radiation at 253.7 nm (Heraeus GPH212T5L/4, 10 W) in the axial position. The optical pathway (1.7 cm) was calculated according to the method developed by Beltran et al. (1995) [45]. Incident photonic flux (I_0) was determined via actinometry experiments using H_2O_2 and atrazine as actinometers [40, 41], the results of which indicated an I_0 of 2.41 J m^{-2} s^{-1}. The reactor was coupled to a cooling system, and temperature was kept constant at 20 °C during reactions.

The UV-C lamp was pre-heated for 20 minutes before each reaction. Once the solution temperature was stabilized at 20 °C, H_2O_2 (commercial grade, 39%) or sodium persulfate (Na_2SO_8, Aldrich) were added to the solution at a concentration

of 10^{-3} M (molar ratio of H_2O_2 or $S_2O_8^{2-}$: target substance 20:1 for CAF, LP, and FRSM, and 32:1 for CBZ). Samples were withdrawn during the reactions for quantification of the target compounds using HPLC, total organic carbon (TOC; TOC-VCSH Total Carbon Analyzer, Shimadzu), and residual H_2O_2 or persulfate, according to previously described procedures [46]. All conditions were tested in duplicate, and the pH was monitored during reactions.

In order to assess the influence of natural scavengers, namely inorganic ions (HCO_3^-, NO_3^-, PO_4^{3-}) and NOM, on the degradation of CECs via UV-C, UV-C/H_2O_2, and UV-C/$S_2O_8^{2-}$, reactions were performed in surface water and ultra-pure water each containing all four target compounds. Both matrices were spiked with a solution containing a mix of the four compounds such that the final concentration of each compound was 10 µM (total CEC_0 concentration = 40 µM). The surface water (SW) used in these experiments was sampled from the Lys River at Aire sur la Lys, France.

2.4 Acute toxicity assays

Acute toxicity analyses were performed using the Microtox® method (Model 500 Analyzer SDI) (ISO 11348-3:2007) on samples withdrawn during UV-C photolysis and the UV-C AOP processes performed in the UV-C reactor, as described previously [47]. *Allivibrio fischeri* was exposed to samples diluted to different degrees, luminescence was measured after 5, 15, and 30 min of exposure, and relative inhibition (EC_{50}, %) was obtained and converted to acute toxicity units (a.T.u.; = $100/EC_{50}$). According to the method employed, samples were considered toxic when the a.T.u. value was above 1.2 (EC_{50} > 81.9%). Catalase (Synth®, 460 mg L^{-1} in 0.04 M phosphate buffer) and ascorbic acid (Merck, 440

187 mg L^{-1}) solutions were used as quenching agents for the consumption of residual
188 hydrogen peroxide and persulfate present in the samples, respectively [48, 49].
189 Neither of these reagents are toxic to *Allivibrio fischeri,* as previously reported
190 [49] and as confirmed experimentally by blank tests. The pH was adjusted (to
191 6.5–7.5) prior to toxicity analysis.

192 2.5 Transformation products (TPs)

193 The samples withdrawn during UV-C and UV-C/AOP treatments were analyzed
194 via direct injection high-resolution electrospray ionization (ESI)-mass
195 spectrometry (Bruker micrOTOF-QII) in negative mode for LP and FRSM, and in
196 positive mode for CAF and CBZ. In order to increase the signal, formic acid was
197 added to the CAF and CBZ samples, and ammonium hydroxide was added to
198 the FRSM and LP samples (both at concentrations at 0.1%). A blank sample
199 containing water and formic acid or ammonium hydroxide was analyzed before
200 each measurement. The transformation products (TPs) obtained from the original
201 substances were proposed by considering two different strategies: a structure
202 showing the exact mass detected by the instrument; or simpler structures
203 considering oxidative radical attack and the energy required to break specific
204 chemical bonds in the original molecule.

205 3. Results and Discussion

206 3.1 Determination of quantum yields

207

208 Figure 1 shows the UV-C photolysis of each target compound at different pH
209 values, and Table 1 presents the quantum yields and C_p values obtained at acidic
210 (pH = 3.0), natural (pH of solution without adjustment), and basic (pH = 9.0) pH.

Figure 1. Photolysis (UV-C_{254nm}) of LP (2.2 µM), FRMS (3.0 µM), CAF (5.2 µM), and CBZ (5.5 µM) in ultrapure water at acidic, natural (non-adjusted), and basic pH (I_0 = 2.54 J m^{-2} s^{-1}, volume 3.5 mL) as a function of incident energy per area (mJ cm^{-2}).

Table 1 – Quantum yields and photolysis coefficients (C_p) obtained for each compound at 254 nm at different pH values.

	$\Phi_{254\ nm}$ (mol Einstein^{-1})			$C_{p\ 254\ nm}$(L Einstein^{-1} cm^{-1})		
pH	3	n	9	3	n	9
LP	0.0115±0.0001	0.0153±0.0001	0.0144±0.0006	123.6	190.2	190.2
FRSM	0.0815±0.0001	0.0294±0.0006	0.0245±0.0006	380.4	95.1	95.1
CAF	0.0007±0.0001	0.0005±0.0002	0.0008±0.0001	4.1	1.9	3.8
CBZ	0.0027±0.0001	0.0016±0.0001	0.0021±0.0001	7.6	4.7	9.5

n = pH of solution without adjustment (6.0 for LP, 5.5 for FRSM, 5.8 for CAF, 7.1 for CBZ). Errors were calculated from duplicate measurements.

Considering the high ε_{254nm} of LP (12 355 M^{-1} cm^{-1}) at pH 6, its degradation by direct UV-C photolysis could have been supposed. The chemical structure of LP (Table S1) consists of two aromatic rings and various unsaturated bonds and functional groups containing nitrogen, all of which are known as absorbers [11], thus explaining the high molar attenuation coefficient (Table S1) [10]. The susceptibility of LP to photolysis at 254 nm in medical formulations based on a drinkable cherry syrup has been reported previously [50, 51]. However, there are no previous reports on the photolysis nor on the values of quantum-yield for LP in water. The quantum yields obtained for LP (Table 1) varied from 0.011 to 0.015 mol Einstein^{-1} (Figure 1, Table 1), and was slightly lower at acidic pH compared to the values obtained at pH 9 and 6 (Figure 1A). The slightly higher molar absorptivity and photolysis coefficients obtained at pH 6 and 9 in comparison to

232 that at pH 3 could be explained by the pKa of this compound (4.15) (Table S1).
233 According to the pKa, LP would exist in its neutral form at pH 3 but in the
234 dissociated form at pH 6 and 9. As the chemical structures of the neutral and the
235 protonated form are distinct, the molar absorptivity may be affected [40].
236 Specifically, it was slightly higher for the dissociated form of LP than for the
237 neutral form, as confirmed by the ε_{254nm} values which increased from 10 700 M^{-1}
238 cm^{-1} at pH 3 to 13 140 M^{-1} cm^{-1} at pH 9 (Table S2).

239 As molar attenuation coefficient is influenced by the dissociated/non-dissociated
240 structure and C_p describes a relation between the quantum yield and the molar
241 attenuation coefficient, the C_p values obtained for LP also varied according to pH
242 (Table 1), specifically being higher at pH 6 and 9 than at pH 3. The C_p obtained
243 for LP is higher than the value of 40 which indicates that a compound is
244 susceptible to direct photolysis [3]. The C_p is also similar to those obtained for
245 atrazine and pentachlorophenol [4]. Atrazine also presents functional groups that
246 contribute to light absorption and photolysis. Although atrazine exhibits a lower
247 ε_{254} (3860 M^{-1} cm^{-1} at pH 7) than LP, atrazine has a higher quantum yield (0.046
248 mol $Einstein^{-1}$). Therefore, these compounds show similar susceptibility to
249 photolysis ($C_{p\ atrazine}$ = 160) [4]. In addition to direct UV-C photolysis, chain
250 reactions may be triggered after a compound undergoes photolysis due to the
251 formation of other radicals in the system, such as Cl• [4]. Considering that LP,
252 atrazine, and pentachlorophenol all contain chlorine atoms in their structures, Cl•
253 radicals may be generated, which would lead to further degradation of these
254 compounds under UV-C irradiation.

255 As shown in Figure S1, FRSM has a lower light absorption coefficient at 254 nm,
256 while it absorbs strongly at 230 nm and 270 nm. In addition, the molar attenuation

coefficients obtained for FRSM at 254 nm ranged from 3200 to 4700 M^{-1} cm^{-1}, corresponding to pH 5.5 and 3, respectively (Table S2). As the pKa of FRSM is 3.9 (Table S1) [52], this compound exists in its neutral form at pH 3, where it exhibited a higher absorptivity and molar attenuation coefficient at 254 nm (Table S2) than at other pH values. As a consequence, photolysis coefficient, and UV-C photolysis of FRSM were higher at acidic pH (Table 1, Figure 1). The photo-instability of FRSM in the neutral form has been previously reported, and the photolysis product showed increased reactivity, solubility in water, and genotoxicity in comparison to the parent compound [53, 54].

As the molar attenuation coefficient (4660 M^{-1} cm^{-1}) of FRSM at 254 nm was highest at pH 3, the photolysis coefficient *Cp* of this compound was more than 3 times higher at pH 3 than at pH 5.8 and 9 (Table 1). The photolysis coefficient of FRSM at pH 3 is comparable to that of the antibiotic sulfamethazine, likely due to the presence of similar functional groups present, such as sulfonamide and chlorobenzene moieties. These functional groups are light absorbers, thus contributing to UV-C photolysis and to the occurrence of secondary chain reactions [4]. Meanwhile, when the solution pH was above the pKa, the absorbance of the dissociated form of the compound was lower (Table S2). Therefore, molar absorptivity and photolysis coefficients were also lower under these conditions. The quantum yield obtained at pH 5.5 for FRSM was 0.0294 mol $Einstein^{-1}$, which is in agreement with previously reported values (0.02200 ± 0.0028 mol $Einstein^{-1}$) [55].

The absorption spectrum (Figure S1) of CAF reveals that absorbance of this compound at 254 nm was reduced when compared to 205 nm and 273 nm, and to the absorbance of LP and FRSM at this wavelength. According to the molar

attenuation coefficients obtained at 254 nm (Table S2), the molar absorptivity of CAF did not change significantly with pH. This suggests that the structure of CAF is not influenced by the pH, which is in agreement with previous reports that the pKa of CAF is either above 10 [56] or “not observable within the pKa scale in water (0-14)” [10] (Table S1). Therefore, photolysis coefficients obtained for CAF in acidic and basic conditions were similar (Table 1). This testifies for the photo-stability of CAF over the tested pH range (Figure 1). The quantum yield obtained for CAF in this study was similar to the value reported in the literature (0.0003 mol Einstein^{-1}) [12]. Carlson et al. [10] also reported insignificant photolysis of caffeine, thus confirming that this compound is not susceptible to UV-C photolysis. As the molar absorptivity was similar at pH 3, 5.5 and 9, the photolysis coefficients of CAF were low in all of the tested pH range, ranging from 1.9 to 4.1 mol Einstein^{-1}. Interestingly, the photolysis coefficients obtained for CAF were similar to those reported for carbamazepine (C_p = 7), which is also resistant to UV-C photolysis [4]. As caffeine and carbamazepine have been increasingly detected in water resources, their low susceptibility to photolysis would call for other alternative methods for their treatment in wastewater effluent or in drinking water treatment processes.

The absorbance of CBZ at 254 nm was relatively low (Figure S1). Thus, UV-C photolysis of this compound was expected to be relatively low in comparison to compounds that absorb strongly at this wavelength, such as LP. The slightly higher molar attenuation coefficients measured at pH 7 and 9 (Table S2), which are above the pKa (4.2), in comparison to that measured at pH 3, indicate that the substance more readily absorbs photons in its dissociated form. Quantum yield values (Table 1) obtained for CBZ confirm the stability of this compound

307 under UV-C irradiation (Figure 1). In addition, the quantum yields shown in Table
308 1 agree with the values reported previously [57, 58]. The slightly higher decay of
309 CBZ observed at pH 9 in comparison to that at pH 3 or 7 is also in agreement
310 with the molar absorptivity values (Table S2). As a consequence of the lower
311 molar attenuation coefficient, the photolysis coefficients of CBZ at different pH
312 are also negligible and comparative to those obtained for CAF. Similarities in the
313 chemical structures (such as the imidazole moiety) of CBZ and CAF may explain
314 the correspondence between the quantum yield and C_p values obtained for both
315 compounds (Table 1, Figures 1C and D). In comparison to other pesticides such
316 as atrazine and alachor, CBZ is much more resistant to photolysis [4]. The higher
317 photolysis of atrazine and alachlor in comparison to CBZ may be related to the
318 de-chlorination of these compounds [59, 60], which does not occur in CBZ since
319 it does not contain chlorine.

320 3.2 Degradation of target compounds via UV-C/H_2O_2 and UV-C/$S_2O_8^{2-}$

321 Profiles of the degradation of target compounds, pH values, and consumption of
322 H_2O_2 and $S_2O_8^{2-}$ over the courses of the UV-C AOP are shown in Figure 2.
323 Control experiments consisted of H_2O_2 or $S_2O_8^{2-}$ in the same concentration
324 without UV-C irradiation, and showed neither removal nor mineralization of target
325 compounds (Figure S2). The use of these oxidants in combination with UV-C
326 irradiation increased the removal of all target compounds, especially for the
327 photo-stable compounds CAF and CBZ, resulting in degradation of over 90%
328 (Figure 2) with a dose of 300 to 600 mJ cm^{-2} of UV irradiation, depending on the
329 target compound.

330

Figure 2. Left: Degradation of each target compound by UV-C AOPs: UV-C/H_2O_2 and UV-C/$S_2O_8^{2-}$. Control experiments are also presented (UV-C photolysis, H_2O_2, or $S_2O_8^{2-}$ alone). Molar ratio of H_2O_2 or $S_2O_8^{2-}$: compound = 20:1 for LP, FRSM, and CAF, and 32:1 for CBZ; I_0 = 2.41 J m^{-2} s^{-1}. Right: consumption (%) of H_2O_2 (C_0 = 10^{-3} M), $S_2O_8^{2-}$ (C_0 = 10^{-3} M), and pH values monitored during UV-C AOPs for each of the target compounds, as functions of incident energy per unit area (mJ cm^{-2}).

Experiments conducted with LP showed that UV-C photolysis alone achieved up to 85% removal in one hour (corresponding to 870 mJ cm^{-2}), while UV-C/$S_2O_8^{2-}$ and UV-C/H_2O_2 reached the same removal rate (Figure 2) after 290 and 620 mJ cm^{-2} incident energy, respectively, both achieving 98% removal by 870 mJ cm^{-2}. UV photolysis of FRSM reached 87% removal after 870 mJ cm^{-2} incident energy, while in the presence of H_2O_2 or $S_2O_8^{2-}$, the same efficiency was achieved with 435 and 650 mJ cm^{-2}, reaching 98% and 93% removal, respectively, after one hour (Figure 2). Degradation rates of FRSM via UV-C only and UV-C/H_2O_2 determined in this study are in agreement with values reported in the literature [61]. After one hour of reaction (total incident energy 870 mJ cm^{-2}), both UV-C AOPs achieved efficient degradation of LP and FRSM, despite the maximum TOC removals being limited to 10% and 6%, respectively (Fig. S2). These results indicate the accumulation of organic transformation products in the system.

The limited consumption of H_2O_2 in the presence of LP and FRSM (10%) (Figure 2) probably occurred as a result of the molar attenuation coefficients of these compounds ($\varepsilon_{254nm,\ LP,\ pH\ 7}$ =11772 M^{-1} cm^{-1}, $\varepsilon_{254nm,\ FRSM,\ pH\ 6}$ = 3700 M^{-1} cm^{-1}) (Table S2) being higher than that of H_2O_2 ($\varepsilon_{254nm,\ H2O2}$ = 19.6 M^{-1} cm^{-1}) [4, 62]. The pharmaceuticals diclofenac and mecoprop, which are strong light absorbers, also impaired the absorption of light by H_2O_2 during UV-C/H_2O_2 treatment [12], thus reducing the process efficiency; this effect is a problem known to occur in the

presence of strong photon absorbers [63]. One other reason for the low consumption of H_2O_2 in these systems, when compared to the consumption of $S_2O_8^{2-}$ (25%), may be related to the lower rate constants for the self-scavenging effects of $SO_4^{-\bullet}$ with $S_2O_8^{2-}$ ($k_{SO4-\bullet/S2O82-}$ = 6:6 x 10^5 M^{-1} s^{-1} and $k_{SO4-\bullet/\ SO4-\bullet}$ = 3:1 x 10^8 M^{-1} s^{-1}) in comparison to those of $HO\bullet$ toward H_2O_2 ($k_{OH/H2O2}$= 2:7 x 10^7 M^{-1} s^{-1} and $k_{OH\bullet/OH\bullet}$= 5:5 x 10^9 M^{-1} s^{-1}) [17, 64, 65].

As shown in Figure 2 (left column), after 200 mJ cm^{-2} of incident energy, the concentrations of LP and FRSM were reduced by a factor of 2. Therefore, competition for light decreased and H_2O_2 and $S_2O_8^{2-}$ consumption subsequently increased (Figure 2, right). However, concentrations of both reagents were still high at this moment since consumption was lower than 5% of initial concentration (9.5 x 10^{-4} M of remaining H_2O_2 and $S_2O_8^{2-}$) (Figure 2, right column). As regeneration of hydrogen peroxide from hydroxyl radicals via self-scavenging occurs more readily than the regeneration of $S_2O_8^{2-}$ from sulfate radicals, the final consumption of H_2O_2 at the end of treatment was limited to a maximum of 10% of initial concentration after 850 mJ cm-^{2} of incident energy, when compared to nearly 30% consumption of $S_2O_8^{2-}$ in the presence of LP and FRSM (Figure 2, right column).

During LP degradation, 30% of initial $S_2O_8^{2-}$ were consumed after 430 mJ cm^{-2} of incident energy (Figure 2, right column), while H_2O_2 consumption was limited to 10%. Assuming stoichiometric conversion of reagents to oxidative radicals 6 x 10^{-4} M of sulfate radicals were generated when compared to 2 x 10^{-4} M of hydroxil radicals, thus explaining the faster LP degradation via UV-C/$S_2O_8^{2-}$ (98% within 430 mJ cm^{-2}) when compared to the degradation via UV-C/H_2O_2 (70% within 430 mJ cm^{-2}) (Figure 2, left). On the other hand, both UV-C AOPs and the UV-C

384 photolysis exhibited similar patterns in terms of FRSM removal and reagent
385 consumption until 220 mJ cm^{-2} of incident energy (Figure 2, left column),
386 suggesting that photolysis was the predominant mechanism in the system, which
387 is supported by the fact that FRSM is a strong light absorber (Section 3.1, Figure
388 1, Table 1). However, after reaching 430 mJ cm^{-2} of incident energy, $S_2O_8^{2-}$
389 consumption reached 21% while only 5% of the initial H_2O_2 had been consumed.
390 Assuming stoichiometric conversions of $S_2O_8^{2-}$ and H_2O_2 to oxidative radicals,
391 nearly 4.2 x 10^{-4} M of sulfate radicals were formed in the system, compared to 10^{-4}
392 M of hydroxyl radicals. However, FRSM degradation via UV-C/H_2O_2 at this
393 moment was 99%, while it was only 80% via UV-C/$S_2O_8^{2-}$ (Figure 2, left column).
394 In contrast with LP, for which the degradation was higher in the UV-C/$S_2O_8^{2-}$
395 system, this result suggests that FRSM is more reactive with hydroxyl radicals
396 than with sulfate radicals, which may be related to differences in the chemical
397 structures [3, 15].

398 CAF and CBZ did not undergo photolysis, which was expected due to their low
399 quantum yields and molar absorption coefficients. In contrast, both UV-C AOPs
400 achieved over 99% removal of CAF and CBZ (Figure 2, left comlumn). CBZ
401 degradation was faster via UV-C/H_2O_2, reaching 99% removal after 290 mJ cm^{-2}
402 of incident energy, in comparison to the 650 mJ cm^{-2} required to achieve similar
403 removal by UV-C/$S_2O_8^{2-}$. Mineralization of CAF and CBZ in the UV-C/$S_2O_8^{2-}$
404 process was more extensive (reaching 60% and 70%, respectively) than it was
405 in the presence of hydroxyl radicals (reaching 25% and 35%, respectively)
406 (Figure S2). The drop in pH from 9 to 8 during UV-C/$S_2O_8^{2-}$ (which was not
407 observed in UV-C/H_2O_2) was due to the formation of SO_4^{2-} and H^+ [16]. Higher
408 mineralization rates through UV-C/$S_2O_8^{2-}$ can likely be explained by the greater

409 selectivity and lifespan of sulfate radicals in comparison to hydroxyl radicals as it
410 is less reactive with inorganic species that may be formed during the degradation
411 of target compounds (O, Cl-, NO_3^- and CO_3^{2-}, HCO_3^{2-}), and also towards $S_2O_8^{2-}$ and
412 sulfate radical itself (self-scavenging), thus increasing its persistence in the
413 system. This was also reported with other compounds such as 2,4-D,
414 carbamazepine, and azathioprine [14, 66-68]. In addition, the ability UV-C/$S_2O_8^{2-}$
415 to degrade carboxylic acids and intermediate products usually formed during
416 oxidation processes has been previously confirmed [16].

417 As CAF and CBZ do not absorb UV-C light as extensively as LP and FRSM,
418 irradiation is promptly absorbed by reagents in the UV-C AOPs, leading to higher
419 and faster degradation when compared to UV-C photolysis (Figure 2, Table 2)
420 and higher consumption of H_2O_2 in the UV-C AOPs, reaching 23% for CAF and
421 30% for CBZ (Figure 2). An increase in pH at the beginning of the reactions was
422 observed during UV-C/H_2O_2 treatments of CAF and CBZ (Figure 2 – right
423 column), which likely contributed to higher consumption of H_2O_2 as cleavage is
424 favored in alkaline conditions [69]. $S_2O_8^{2-}$ consumption exhibited similar behavior
425 to that of H_2O_2 during the degradation of CAF and CBZ.

426 Degradation data obtained during UV-C AOPs were fitted to a pseudo-first-order
427 kinetics model ($R^2 > 0.95$), and apparent rate constants were calculated for each
428 process for the different target compounds (Table 2). Electrical energy per order
429 of removal (EE/O; kWh m^{-3}) was also calculated in order to compare the
430 efficiencies of the different processes (Table 2). EE/O values represent the
431 amount of energy required to decrease the concentration of the compound by
432 one order of magnitude [66]. Therefore, higher k'_{app} values result in lower EE/O
433 values, revealing the most efficient process in terms of lowest energy

consumption [70]. However, EE/O should not be considered alone when aiming to identify the most affordable process; reagent costs must also be considered, as, for example, persulfate is more expensive than H_2O_2 [71]. When compared to UV-C photolysis alone, k'_{app} values increased in the presence of hydroxyl and sulfate radicals. Regarding UV-C photolysis, the EE/O values (Table 2) were calculated using experimental data for FRSM, as this process reduced the concentration of this compound by one order of magnitude within 650 mJ cm^{-2} of incident energy. In contrast, for LP, EE/O values were predicted using the $k'_{UV\text{-}C}$ obtained for this compound. As UV-C photolysis of CAF and CBZ did not fit the pseudo-first-order model ($R^2 < 0.95$), it was not possible to estimate EE/O values for the photolysis of these compounds. Apparent rate constants values for the degradation of CAF via UV-C/H_2O_2 agree with the values obtained by Shu et al. [12], who reported higher values of these constants for compounds with reduced quantum yields (caffeine and carbamazepine). Therefore, data on the photolysis coefficients and quantum yields of emerging contaminants present in water may be a valuable tool to predict their degradability via UV-C photolysis, or whether UV-C AOPs would need to be applied [3].

Apparent rate constants obtained for the UV-C/H_2O_2 process were higher than those of the UV-C/$S_2O_8^{2-}$ process for all target compounds except LP. This is likely due to the higher reaction rate of this compound with sulfate radical than with the hydroxyl radical. A decrease in the concentration of LP by one order of magnitude occurred after 20 minutes (290 mJ cm^{-2} of incident energy) for UV-C/$S_2O_8^{2-}$ (Figure 2), yet 45 minutes (650 mJ cm^{-2}) were required to achieve the same removal (Table 2) by UV-C/H_2O_2, as reflected in the k'_{app} and EE/O values. The lower k'_{app} values obtained for UV-C/$S_2O_8^{2-}$ compared to that of UV-C/H_2O_2

during the degradation of FRSM, CAF, and CBZ may be related to the higher selectivity of SO_4^{-}• when compared to that of HO•, since it acts preferentially via electron transfer whereas HO• also reacts via addition and H-abstraction [72]. UV-C/H_2O_2 required 20 minutes (290 mJ cm^{-2}) to reduce the FRSM concentration by one order of magnitude, while 45 minutes (650 mJ cm^{-2}) were required by UV-C/$S_2O_8^{2-}$, thus explaining the higher EE/O of the former process (Table 2).

Table 2 – Pseudo-first-order rate constants (min^{-1}) obtained for each process for the different target compounds, and EE/O values obtained for UV-C/H_2O_2 and UV-C/$S_2O_8^{2-}$ for the different target compounds

Pseudo-first-order rate constant (*k';* min^{-1})	LP	FRSM	CAF	CBZ
$k'_{UV\text{-}C}$	0.011±0.005	0.056±0.004	*	*
$k'_{UV\text{-}C/H2O2}$	0.048±0.0003	0.11±0.01	0.100±0.001	0.22±0.01
$k'_{UV\text{-}C/S2O82-}$	0.0864±0.0005	0.072±0.002	0.085±0.007	0.17±0.04
EE/O (kWh m^{-3})				
UV-C	2.3 P**	1.5 P		
UV-C/H_2O_2	1.5 P	0.67 P	0.5 P	0.25 P
UV-C/$S_2O_8^{2-}$	0.6 P	1.5 P	0.5 P	0.33 P

*Did not fit the model due to low degradation ($R^2 < 0.95$). P is the lamp power (10 W)
**Estimated using the $k'_{UV\text{-}C}$ value.

The EE/O values obtained for CAF degradation were the same for both UV-C AOPs (0.5 P), indicating that the energy required to remove this compound in water using either H_2O_2 or $S_2O_8^{2-}$ under UV-C irradiation was the same. This result agrees with the similarity between the kinetic rates obtained for each process (Table 2). For CBZ, both UV-C AOPs showed comparable k'_{app} and EE/O values (Table 2). The degradation of carbamazepine, another photo-resistant compound, via UV-C/H_2O_2 and UV-C/$S_2O_8^{2-}$ also led to similar EE/O values in a previous study [22]. Indeed, the quantum yield, photolysis coefficient, molar mass, and chemical composition of CAF and CBZ are all very similar, which might explain their comparable behavior when submitted to UV-C AOPs.

3.4 Evolution of acute toxicity

As shown in Figure 3, acute toxicity varied between treatments for all compounds, indicating the formation of toxic intermediates during UV-C AOPS, as has been reported in the literature for various emerging contaminants [23]. The LP solution was not toxic to *Allivibrio fischeri (a.T.u. = 0.26)*, and no acute toxicity was observed during UV-C/H_2O_2 treatment. However, acute toxicity developed during the UV-C-only and UV-C/$S_2O_8^{2-}$ processes, despite the high degradation efficiencies achieved during these processes (65% for UV-C and 98% for UV-C/$S_2O_8^{2-}$). According to Adachi et al. [73], the cyanide ion is formed when LP is oxidized by sodium hypochlorite. Therefore, this ion could have been formed by oxidation during the UV-C AOPs, which may have contributed to the increase in acute toxicity. This difference between the degradation by sulfate and by hydroxyl radicals have been described in previous studies [24]. However, there is no report in the literature regarding the formation of toxic transformation products during UV-C photolysis and UV-C/$S_2O_8^{2-}$ oxidation of LP, nor of other sartans with similar structures. In contrast, the EE/O values suggest that UV-C/$S_2O_8^{2-}$ is more efficient than UV-C/H_2O_2 in the removal of LP. This result indicates that it is not adequate to consider the EE/O values alone for identifying the optimal treatment method.

Figure 3. Acute toxicity of samples withdrawn during the degradation of target compounds via UV-C, UV-C/H_2O_2, and UV-C/$S_2O_8^{2-}$ processes, shown as functions of the total incident energy received (mJ cm^{-2}). The horizontal lines represent the threshold of 1.21 a.T.u.; bars crossing the line thus indicate toxic samples.

FRSM was reported to be non-toxic to *Allivibrio fischeri* [54], yet its products of

505 photolysis and electro-Fenton degradation are considered toxic [74, 75]. In the
506 present study, before treatment, the FRSM solution exhibited a beneficial
507 stimulatory effect, known as hormesis, upon the photobacteria (Figure 3). This
508 effect occurs with luminescent bacteria as a consequence of exposure to small
509 concentrations of toxic chemicals [76]. As shown in Figure 3, acute toxicity was
510 generated during the UV-C photolysis of FRSM, but was eliminated within 600
511 mJ cm^{-2} of incident energy, when this process reached FRSM removal of 80%
512 (Figure 2). Meanwhile, there was no generation of toxicity during the UV-C/H_2O_2
513 process. In contrast, UV-C/$S_2O_8^{2-}$ exhibited similar behavior to the UV-C-only
514 process, as toxicity was generated at the beginning of the reaction but was
515 eliminated within 300 mJ cm^{-2} of incident energy, much less than that required
516 with the UV-C-only process (Figure 3).

517 Before treatment, the CAF solution exhibited an inhibitory effect (Ec_{50} = 76%;
518 a.T.u. = 1.3) on *Allivibrio fischeri*, as has been reported for similar tests using a
519 marine photobacterium as a bioindicator (Ec_{50} = 62.8%) [77]. Although a few
520 authors reported that there was no increase in CAF toxicity after AOP treatments
521 [78, 79], no reports on the effect of UV-C/H_2O_2 or UV-C/$S_2O_8^{2-}$ on CAF toxicity
522 have been published. This is alarming since caffeine is detected in surface waters
523 in a wide variety of locations in concentrations up to µg L^{-1} [34], and was even
524 considered for use as an indicator of illegal sewage disposal [37]. Both UV-
525 C/H_2O_2 and UV-C/$S_2O_8^{2-}$ increased CAF toxicity at the beginning of the treatment,
526 although the toxic effects were entirely eliminated toward the end of the
527 treatments when the concentration of CAF was below 10% of its initial
528 concentration (Figure 3). This suggests the formation and degradation of toxic
529 transformation products within both processes. With regards to UV-C photolysis,

for which only the final sample was analyzed due to the negligible effect of this process on the removal of CAF, an increase in toxicity during treatment was also observed.

As confirmed by the results shown in Figure 3, CBZ is known to be toxic to *Allivibrio fischeri [80]*. Similarly to what was observed for CAF, UV-C photolysis alone was not able to remove CBZ due to its low molar absorptivity and quantum yield. Consequently, UV-C photolysis had a negligible effect on the acute toxicity of CBZ. Meanwhile, both UV-C/H_2O_2 and UV-C/$S_2O_8^{2-}$ eliminated the toxic effect of CBZ; as it was also observed by other irradiated AOPs under artificial and solar irradiation in another study [80]. During UV-C/H_2O_2, CBZ degradation occurred alongside the reduction in acute toxicity (Figure 3). In contrast, acute toxicity increased during the initial stages of the UV-C/$S_2O_8^{2-}$ process and decreased toward the end, probably due to the formation of toxic transformation products. This result agrees with the EE/O values (Table 2), as less energy was required to reduce the toxicity of CBZ via UV-C/H_2O_2 compared to UV-C/$S_2O_8^{2-}$.

3.5 Degradation of target compounds by UV-C/H_2O_2 and UV-C/$S_2O_8^{2-}$ in surface water

In order to assess the impact of the water matrix on the degradation of target compounds, UV-C, UV-C/H_2O_2, and UV-C/ $S_2O_8^{2-}$ treatments were applied to surface water and ultrapure water each spiked with 10 µM of each compound. Although degradation of all compounds occurred simultaneously, since all compounds were present in the same matrix, the degradation of each pollutant was quantified individually (Figure 3). Reduction in TOC and consumption of H_2O_2 and $S_2O_8^{2-}$ were also monitored (Figure 4).

Figure 4. Degradation of LP, FRSM, CAF, and CBZ (10 µM each) in ultra-pure water and surface water by UV-C, UV-C/H_2O_2, and UV-C/$S_2O_8^{2-}$ processes ($C_{0H2O2 \text{ or } S2O82-}$ = 10^{-3} M), shown as functions of total incident energy per area (mJ cm^{-2}).

The presence of scavenger compounds that are naturally present in real surface water, including HCO_3^-, natural organic matter (NOM), and Cl^-, among others, may lead to a lower degradation of target compounds in practical applications [70]. NOM is mainly comprised of humic acids which present various functional groups that compete with the target compounds for hydroxyl and sulfate radicals [81, 82]. As shown in Figure 4, UV-C photolysis of CBZ in the surface water and in the presence of the other target compounds was similar to that observed in pure water, still exhibiting an insignificant decrease in concentration due to its lower quantum yield and molar absorptivity at 254 nm (Table 1). On the other hand, the UV-C photolysis of each of LP, FRSM, and CAF was slightly higher in surface water than in pure water. This likely happened due the formation of oxidative radicals from the natural constituents of the Lys River surface water, which presented a DOC of 1.2 mg L^{-1}; O_2 concentration 8 mg L^{-1}; NO_3^- concentration 22 mg L^{-1}; PO_4^{3-} concentration 0.1 mg L^{-1}; Cl^- concentration 20 mg L^{-1}; and high alkalinity of 330 mg L^{-1} HCO_3^-. A greater extent of photolysis of FRSM in natural waters than in pure water was also observed previously [61]. When NOM, dissolved oxygen, and phosphate are submitted to UV-C_{254nm} irradiation, oxidative species such as NOM•, singlet oxygen ($^1O_2$), and PO_4^{2-}• may be formed [83, 84]. Although these radicals present lower redox potentials than HO• and SO_4^-•, they may have contributed to the enhanced photolysis of LP, FRSM, and CAF [85]. Further, HO• may also be formed from the irradiation of

581 NO_3^- present in surface waters [86, 87].

582 Lower degradations of LP and FRSM were observed during UV-C AOPs in
583 surface water than in pure water. The high level of carbonate ions in surface water
584 may have contributed to the quenching of hydroxyl and sulfate radicals involved
585 in the degradation reactions. In contrast, for CAF and CBZ, the effect of matrix
586 constituents on the oxidative radicals formed during the UV-C AOPs could not be
587 observed, probably because their reaction rates with radicals are extremely high,
588 as shown in Table 2. The relatively high content of chloride ions, which react
589 strongly with sulfate radicals [88], may have influenced the effectiveness of the
590 UV-C/$S_2O_8^{2-}$ process, thus leading to the lower removal of target compounds in
591 surface water than in pure water.

592 The consumption rates of H_2O_2 and $S_2O_8^{2-}$ were below 25% in all of the tested
593 conditions (Figure 5). H_2O_2 consumption in pure water was 13%, but 20% in
594 surface water, thus confirming that a higher consumption of this reagent occurred
595 in the presence of other matrix components. On the other hand, $S_2O_8^{2-}$
596 consumption was very similar in pure water (20%) and in the presence of matrix
597 components (24%). In addition, previous studies have confirmed that the
598 performance of the UV-C/$S_2O_8^{2-}$ process is not disturbed by carbonate ions
599 (HCO_3^-) to such an extent as is the performance of the UV-C/H_2O_2 process,
600 probably due to the lower reaction constants for the reaction of $SO_4^{-\bullet}$ with HCO_3^-
601 ($k_{SO4^{\bullet-},\,HCO3} = 2.8 \times 10^6\ M^{-1}\ s^{-1}$) than that of OH• with HCO_3^- ($k_{HO^\bullet,\,HCO3} = 8.5 \times 10^6$
602 $M^{-1}\ s^{-1}$) [6, 14, 17-19]. Furthermore, the TOC removal (Figure 5) achieved by UV-
603 C/$S_2O_8^{2-}$ (9% and 21% in pure water and surface water, respectively) was higher
604 than that achieved by UV-C/H_2O_2 (5.7 and 14.9%, respectively) in both water
605 matrices, thus corroborating the results reported earlier in this study (Section 3.3).

606 The higher mineralization efficiency in surface water than in pure water
607 corresponds to the degradation of NOM via sulfate radicals, as reported
608 previously [65].

609

610 Figure 5. Reagent consumption and TOC removal during UV-C AOPs in surface
611 water (filled symbols) and pure water (empty symbols), as functions of total
612 incident energy per area (mJ cm^{-2}) (Initial TOC in pure water 5.4 mg L^{-1} and in
613 surface water 6.6 mg L^{-1}).

614

615 3.3 Identification of transformation products

616 The mass spectra of CAF before UV-C radiation (zero min) shows two peaks:
617 protonated caffeine **I** ([caffeine+H^+], *m/z* = 195.08) and another signal
618 ([caffeine+Na^+], *m/z* = 217.07) which refers to the sodium adduct (Figure 6A). The
619 peak intensities corresponding to the transformation products detected during
620 CAF oxidation, along with the mass spectra after 315 mJ cm^{-2} of incident energy
621 in the UV-C/H_2O_2 (Figures 6B and C) and UV-C/$S_2O_8^{2-}$ (Figures 6D and E)
622 processes show that a higher number of transformation products were formed
623 during UV-C/H_2O_2 than during UV-C/$S_2O_8^{2-}$, likely due to the higher selectivity of
624 the sulfate radical than the hydroxyl radical. The oxidation of the six-membered
625 ring in UV-C/H_2O_2 first generated 2 main species which presented masses *m/z* =
626 125.98 and 142.06 (Figures 6B and C, at 50 mJ cm^{-2}, and Figure 7), with smaller
627 peaks corresponding to *m/z* 128.02 and 168.04 (Figures 6B and C and Figure 7).
628 However, after 300 mJ cm^{-2} of incident energy, species with *m/z* = 110.01,
629 128.02, and 146.03 were identified in the UV-C/H_2O_2 system (Figures 6B and C
630 and Figure 7).

Figure 6. Mass spectra of (A) Caffeine solution in pure water, (B and D) signals corresponding to masses detected during UV-C/H_2O_2 and UV-C/$S_2O_8^{2-}$ treatments, and (C and E) mass spectra obtained after UV-C/H_2O_2 and UV-C/$S_2O_8^{2-}$ treatments with 300 mJ cm^{-2} of total incident energy.

Meanwhile, the transformation products accumulated during UV-C/ $S_2O_8^{2-}$ were different (*m/z* = 164.92 and 142.94; Figures 6D and E), thus suggesting a different transformation pathway which has not yet been reported for caffeine in the literature. These results are very relevant considering that the use of caffeine as an indicator of so-called 'fresh' contamination of surface waters has been suggested by some authors [35-37].

Considering the spectra obtained during the degradation of CAF via UV-C/H_2O_2, a possible degradation route was proposed, as shown in Figure 7. The signal at *m/z* = 195.09 (structure **I**) corresponds to the protonated adduct of caffeine. The oxidation process led to a decrease in intensity of the *m/z* = 195 signal and increases in the intensities of other signals associated to products of oxidation. ChemCalc [89] was used to assign a formula to the exact mass and then propose a structure based on these formulae. The two first products (**II**: *m/z* = 142.06 and **III**: *m/z* = 125.98) would be formed from a break of the pyrimidine moiety and the opening of the imidazole ring (Figure 7). A signal of *m/z* 142 was also detected by Dalmazio et al., (2005) [90] during the degradation of caffeine via UV-C/H_2O_2. However, considering the exact mass obtained here, the product proposed in the referred paper was not realistic in our case. Species *of m/z* 128.02 (**III**) and 146.03 (**IV**) would be formed from the further oxidation of **II**, leading to an isocyanate structure [80] and the formation of carboxylic acid moieties. Then, compound **VI** would later accumulate in the system as a product of oxidation of the intermediate compounds. However, no structure could be proposed for the

658 detected signals. No structures were proposed for the oxidation products of the
659 UV/$S_2O_8^{2-}$ process, as the formulae proposed for the mass obtained were not
660 relevant for the process [89].

661 Figure 7. Degradation pathway proposed for the formation of transformation
662 products generated during the oxidation of caffeine via UV-C/H_2O_2

663

664 These analyses were also performed with samples withdrawn during the
665 oxidation of LP, FRSM, and CBZ via UV-C/H_2O_2 and UV-C/$S_2O_8^{2-}$. However, as
666 shown in Figures S3, S4, and S5, decreases in the signal intensities of the target
667 compounds were observed, yet no other signals of significant intensity were
668 detected. TPs could not be observed using this methodology as they would not
669 have been ionized by the ESI used here.

670 4. Conclusion

671 In this study, the quantum yields and photolysis coefficients were calculated for
672 target compounds, indicating that LP and FRSM are susceptible to photolysis in
673 the UV-C range (80% removal of each LP and FRSM under UV-C photolysis
674 alone at total levels of 800 and 600 mJ cm^{-2} incident energy). In contrast, the UV-
675 C photolysis of both CAF and CBZ by this process was negligible. UV-C/H_2O_2
676 and UV-C/$S_2O_8^{2-}$ were extremely effective in the removal of all target compounds,
677 achieving over 90% degradation in a pure water matrix under the same
678 conditions. k'_{app} rates were obtained for UV-C/H_2O_2 on the degradation of FRSM,
679 CAF, and CBZ, when compared to UV-C/ $S_2O_8^{2-}$ due to the reactivity of hydroxyl
680 radicals toward these compounds and their intermediates. On the other hand,
681 mineralization rates and reagent consumption were higher in the UV-C/$S_2O_8^{2-}$
682 system, probably due to the greater light absorption and lower self-scavenging

683 exhibited by sulfate radicals as compared to hydroxyl radicals. During acute
684 toxicity analysis using *Allivibrio fischeri*, samples withdrawn during the UV-C-only
685 and UV-C/$S_2O_8^{2-}$ processes exhibited higher toxicity than those withdrawn during
686 the UV-C/H_2O_2 process. Simultaneous degradation of target compounds in real
687 surface water indicated higher stability of the UV-C/$S_2O_8^{2-}$ system in the presence
688 of natural scavengers in comparison to that of the UV-C/H_2O_2 system. A lower
689 number of transformation products were detected during CAF degradation via
690 UV-C/$S_2O_8^{2-}$ as compared to UV-C/H_2O_2, confirming the higher selectivity of the
691 sulfate radical than the hydroxyl radical, and suggesting distinct reaction
692 mechanisms for each radical.

693 Acknowledgments

694 The authors would like to acknowledge Erasmus iBrasil, DOC2C's Interreg 2seas
695 Project, CPER Climibio, Conselho Nacional de Desenvolvimento Científico e
696 Tecnológico (CNPQ), Coordenação de Aperfeiçoamento Profissional de Nível
697 Superior (CAPES), and Fundação de Amparo à Pesquisa do Estado de Minas
698 Gerais (FAPEMIG) for the funding.

699 References

700 [1] S. Giannakis, M. Voumard, D. Grandjean, A. Magnet, L.F. De Alencastro, C. Pulgarin,
701 Micropollutant degradation, bacterial inactivation and regrowth risk in wastewater effluents:
702 Influence of the secondary (pre)treatment on the efficiency of Advanced Oxidation Processes,
703 Water Research 102 (2016) 505-515.
704 [2] E.A. Serna-Galvis, F. Ferraro, J. Silva-Agredo, R.A. Torres-Palma, Degradation of highly
705 consumed fluoroquinolones, penicillins and cephalosporins in distilled water and simulated
706 hospital wastewater by UV254 and UV254/persulfate processes, Water Research 122 (2017)
707 128-138.
708 [3] D. Gerrity, Y. Lee, S. Gamage, M. Lee, A.N. Pisarenko, R.A. Trenholm, U. von Gunten, S.A.
709 Snyder, Emerging investigators series: prediction of trace organic contaminant abatement with
710 UV/H2O2: development and validation of semi-empirical models for municipal wastewater
711 effluents, Environmental Science: Water Research & Technology 2 (2016) 460-473.

712 [4] D.R. Hokanson, K. Li, R.R. Trussell, A photolysis coefficient for characterizing the response of
713 aqueous constituents to photolysis, Frontiers of Environmental Science & Engineering 10 (2016)
714 428-437.
715 [5] J.C. Kruithof, P.C. Kamp, B.J. Martijn, UV/H2O2 Treatment: A Practical Solution for Organic
716 Contaminant Control and Primary Disinfection, Ozone: Science & Engineering 29 (2007) 273-
717 280.
718 [6] C. Luo, J. Ma, J. Jiang, Y. Liu, Y. Song, Y. Yang, Y. Guan, D. Wu, Simulation and comparative
719 study on the oxidation kinetics of atrazine by UV/H2O2, UV/HSO5− and UV/S2O82−, Water
720 Research 80 (2015) 99-108.
721 [7] M.A. Tarr, Chemical Degradation Methods for Wastes and Pollutantes, New York, 2003.
722 [8] G. Boczkaj, A. Fernandes, Wastewater treatment by means of advanced oxidation processes
723 at basic pH conditions: A review, Chemical Engineering Journal 320 (2017) 608-633.
724 [9] M.A. Oturan, J.-J. Aaron, Advanced Oxidation Processes in Water/Wastewater Treatment:
725 Principles and Applications. A Review, Critical Reviews in Environmental Science and Technology
726 44 (2014) 2577-2641.
727 [10] J.C. Carlson, M.I. Stefan, J.M. Parnis, C.D. Metcalfe, Direct UV photolysis of selected
728 pharmaceuticals, personal care products and endocrine disruptors in aqueous solution, Water
729 Research 84 (2015) 350-361.
730 [11] R.F. Dantas, O. Rossiter, A.K.R. Teixeira, A.S.M. Simões, V.L. da Silva, Direct UV photolysis of
731 propranolol and metronidazole in aqueous solution, Chemical Engineering Journal 158 (2010)
732 143-147.
733 [12] Z. Shu, J.R. Bolton, M. Belosevic, M. Gamal El Din, Photodegradation of emerging
734 micropollutants using the medium-pressure UV/H2O2 Advanced Oxidation Process, Water
735 Research 47 (2013) 2881-2889.
736 [13] M. Muruganandham, R.P.S. Suri, S. Jafari, Sillanp, #xe4, M. , G.-J. Lee, J.J. Wu, M.
737 Swaminathan, Recent Developments in Homogeneous Advanced Oxidation Processes for Water
738 and Wastewater Treatment, International Journal of Photoenergy 2014 (2014) 21.
739 [14] Y. Zhang, J. Zhang, Y. Xiao, V.W.C. Chang, T.-T. Lim, Kinetic and mechanistic investigation of
740 azathioprine degradation in water by UV, UV/H2O2 and UV/persulfate, Chemical Engineering
741 Journal 302 (2016) 526-534.
742 [15] M.-S. Tsao, W.K. Wilmarth, The Aqueous Chemistry of Inorganic Free Radicals. I. The
743 Mechanism of the Photolytic Decomposition of Aqueous Persulfate Ion and Evidence Regarding
744 the Sulfate–Hydroxyl Radical Interconversion Equilibrium, The Journal of Physical Chemistry 63
745 (1959) 346-353.
746 [16] J. Criquet, N.K.V. Leitner, Degradation of acetic acid with sulfate radical generated by
747 persulfate ions photolysis, Chemosphere 77 (2009) 194-200.
748 [17] G.V. Buxton, C.L. Greenstock, W.P. Helman, A.B. Ross, Critical Review of rate constants for
749 reactions of hydrated electrons, hydrogen atoms and hydroxyl radicals (·OH/·O− in Aqueous
750 Solution, Journal of Physical and Chemical Reference Data 17 (1988) 513-886.
751 [18] O.P. Chawla, R.W. Fessenden, Electron spin resonance and pulse radiolysis studies of some
752 reactions of peroxysulfate (SO4.1,2), The Journal of Physical Chemistry 79 (1975) 2693-2700.
753 [19] M.G. Antoniou, H.R. Andersen, Comparison of UVC/S2O82− with UVC/H2O2 in terms of
754 efficiency and cost for the removal of micropollutants from groundwater, Chemosphere 119
755 (2015) S81-S88.
756 [20] S. Wacławek, H.V. Lutze, K. Grübel, V.V.T. Padil, M. Černík, D.D. Dionysiou, Chemistry of
757 persulfates in water and wastewater treatment: A review, Chemical Engineering Journal 330
758 (2017) 44-62.
759 [21] Y. Yang, J.J. Pignatello, J. Ma, W.A. Mitch, Effect of matrix components on UV/H2O2 and
760 UV/S2O82− advanced oxidation processes for trace organic degradation in reverse osmosis
761 brines from municipal wastewater reuse facilities, Water Research 89 (2016) 192-200.

[22] L. Lian, B. Yao, S. Hou, J. Fang, S. Yan, W. Song, Kinetic Study of Hydroxyl and Sulfate Radical-Mediated Oxidation of Pharmaceuticals in Wastewater Effluents, Environmental Science & Technology 51 (2017) 2954-2962.
[23] A. Sharma, J. Ahmad, S.J.S. Flora, Application of advanced oxidation processes and toxicity assessment of transformation products, Environmental Research 167 (2018) 223-233.
[24] Y. Yang, X. Lu, J. Jiang, J. Ma, G. Liu, Y. Cao, W. Liu, J. Li, S. Pang, X. Kong, C. Luo, Degradation of sulfamethoxazole by UV, UV/H2O2 and UV/persulfate (PDS): Formation of oxidation products and effect of bicarbonate, Water Research 118 (2017) 196-207.
[25] K. Yin, L. Deng, J. Luo, J. Crittenden, C. Liu, Y. Wei, L. Wang, Destruction of phenicol antibiotics using the UV/H2O2 process: Kinetics, byproducts, toxicity evaluation and trichloromethane formation potential, Chemical Engineering Journal 351 (2018) 867-877.
[26] T. Olmez-Hanci, I. Arslan-Alaton, D. Dursun, B. Genc, D.G. Mita, M. Guida, L. Mita, Degradation and toxicity assessment of the nonionic surfactant Triton™ X-45 by the peroxymonosulfate/UV-C process, Photochemical & Photobiological Sciences 14 (2015) 569-575.
[27] Q. Zhang, J. Chen, C. Dai, Y. Zhang, X. Zhou, Degradation of carbamazepine and toxicity evaluation using the UV/persulfate process in aqueous solution, Journal of Chemical Technology & Biotechnology 90 (2015) 701-708.
[28] E.S. Gonçalves, OCORRÊNCIA E DISTRIBUIÇÃO DE FÁRMACOS, CAFEÍNA E BISFENOL-A EM ALGUNS CORPOS HÍDRICOS NO ESTADO DO RIO DE JANEIRO, Departamento de Geociências da Universidade Federal Fluminense, Universidade Federal Fluminense, Niterói, RJ, 2012, pp. 197.
[29] T. Heberer, Tracking persistent pharmaceutical residues from municipal sewage to drinking water, Journal of Hydrology 266 (2002) 175-189.
[30] D.G.J. Larsson, C. de Pedro, N. Paxeus, Effluent from drug manufactures contains extremely high levels of pharmaceuticals, Journal of Hazardous Materials 148 (2007) 751-755.
[31] C.D.S. Pereira, L.A. Maranho, F.S. Cortez, F.H. Pusceddu, A.R. Santos, D.A. Ribeiro, A. Cesar, L.L. Guimarães, Occurrence of pharmaceuticals and cocaine in a Brazilian coastal zone, Science of The Total Environment 548 (2016) 148-154.
[32] M.A. Sousa, C. Gonçalves, V.J.P. Vilar, R.A.R. Boaventura, M.F. Alpendurada, Suspended TiO2-assisted photocatalytic degradation of emerging contaminants in a municipal WWTP effluent using a solar pilot plant with CPCs, Chemical Engineering Journal 198 (2012) 301-309.
[33] F. Stuer-Lauridsen, M. Birkved, L.P. Hansen, H.C. Holten Lützhøft, B. Halling-Sørensen, Environmental risk assessment of human pharmaceuticals in Denmark after normal therapeutic use, Chemosphere 40 (2000) 783-793.
[34] M.C.V.M. Starling, C.C. Amorim, M.M.D. Leão, Occurrence, control and fate of contaminants of emerging concern in environmental compartments in Brazil, Journal of Hazardous Materials (2018).
[35] S. Froehner, W. Piccioni, K.S. Machado, M.M. Aisse, Removal Capacity of Caffeine, Hormones, and Bisphenol by Aerobic and Anaerobic Sewage Treatment, Water, Air, & Soil Pollution 216 (2011) 463-471.
[36] C.C. Montagner, W.F. Jardim, P.C. Von der Ohe, G.A. Umbuzeiro, Occurrence and potential risk of triclosan in freshwaters of São Paulo, Brazil—the need for regulatory actions, Environmental Science and Pollution Research 21 (2014) 1850-1858.
[37] F.F. Sodré, M.A.F. Locatelli, W.F. Jardim, Occurrence of Emerging Contaminants in Brazilian Drinking Waters: A Sewage-To-Tap Issue, Water, Air, and Soil Pollution 206 (2010) 57-67.
[38] M.K. Burkhardt, T.; Hean, S.; Schmid, P.; Haag, R.; Rossi, L.; Boller, M., Release of biocides from urban areas into aquatic systems, 6th International conference on sustainable techniques and strategies in urban water management (NOVATECH)Lyon, France, 2007.
[39] M. Loewy, V. Kirs, G. Carvajal, A. Venturino, A.M. Pechen de D'Angelo, Groundwater contamination by azinphos methyl in the Northern Patagonic Region (Argentina), Science of The Total Environment 225 (1999) 211-218.

[40] S. Canonica, L. Meunier, U. von Gunten, Phototransformation of selected pharmaceuticals during UV treatment of drinking water, Water Research 42 (2008) 121-128.
[41] I. Nicole, J. De Laat, M. Dore, J.P. Duguet, C. Bonnel, Utilisation du rayonnement ultraviolet dans le traitement des eaux: mesure du flux photonique par actinometrie chimique au peroxyde d'hydrogene, Water Research 24 (1990) 157-168.
[42] J.F.F. ANDERSON, M.C.G. GERLIN, R.A. SVERSUT, L.C.S. OLIVEIRA, A.K. SINGH, M.S. AMARAL, N.M. KASSAB, Development and Validation of an Isocratic HPLC Method for Simultaneous Determination of Quaternary Mixtures of Antihypertensive Drugs in Pharmaceutical Formulations Acta Chromatographica 29(2017) (2016) 95–110.
[43] EPA, Method 631: The Determination of Benomyl and Carbendazim in Municipal and Industrial Wastewater in: EPA (Ed.), EPA, 1993.
[44] EPA, Method 1694: Pharmaceuticals and Personal Care Products in Water, Soil, Sediment, and Biosolids by HPLC/MS/MS EPA, 2007.
[45] F.J. Beltran, G. Ovejero, J.F. Garcia-Araya, J. Rivas, Oxidation of Polynuclear Aromatic Hydrocarbons in Water. 2. UV Radiation and Ozonation in the Presence of UV Radiation, Industrial & Engineering Chemistry Research 34 (1995) 1607-1615.
[46] V.M. Amin, N.F. Olson, Spectrophotometric Determination of Hydrogen Peroxide in Milk1, Journal of Dairy Science 50 (1967) 461-464.
[47] M.C.V.M. Starling, L.A.S. Castro, R.B.P. Marcelino, M.M.D. Leão, C.C. Amorim, Optimized treatment conditions for textile wastewater reuse using photocatalytic processes under UV and visible light sources, Environmental Science and Pollution Research 24 (2017) 6222-6232.
[48] A.J. Poole, Treatment of biorefractory organic compounds in wool scour effluent by hydroxyl radical oxidation, Water Research 38 (2004) 3458-3464.
[49] T. Olmez-Hanci, I. Arslan-Alaton, D. Dursun, Investigation of the toxicity of common oxidants used in advanced oxidation processes and their quenching agents, Journal of Hazardous Materials 278 (2014) 330-335.
[50] S. Kollipara, G. Bende, Y. Bansal, R. Saha, Stability-indicating Reversed-phase Liquid Chromatographic Method for Simultaneous Determination of Losartan Potassium and Ramipril in Tablets, Indian Journal of Pharmaceutical Sciences 74 (2012) 201-210.
[51] R.A. Seburg, J.M. Ballard, T.-L. Hwang, C.M. Sullivan, Photosensitized degradation of losartan potassium in an extemporaneous suspension formulation, Journal of Pharmaceutical and Biomedical Analysis 42 (2006) 411-422.
[52] S.J. Khan, J.E. Ongerth, Modelling of pharmaceutical residues in Australian sewage by quantities of use and fugacity calculations, Chemosphere 54 (2004) 355-367.
[53] D.E. Moore, C.D. Burt, PHOTOSENSITIZATION BY DRUGS IN SURFACTANT SOLUTIONS, Photochemistry and Photobiology 34 (1981) 431-439.
[54] M. Isidori, A. Nardelli, A. Parrella, L. Pascarella, L. Previtera, A multispecies study to assess the toxic and genotoxic effect of pharmaceuticals: Furosemide and its photoproduct, Chemosphere 63 (2006) 785-793.
[55] B.A. Wols, D.J.H. Harmsen, E.F. Beerendonk, C.H.M. Hofman-Caris, Predicting pharmaceutical degradation by UV (LP)/H2O2 processes: A kinetic model, Chemical Engineering Journal 255 (2014) 334-343.
[56] D.W. Newton, R.B. Kluza, pKa Values of Medicinal Compounds in Pharmacy Practice, Drug Intelligence & Clinical Pharmacy 12 (1978) 546-554.
[57] R. Panadés, A. Ibarz, S. Esplugas, Photodecomposition of carbendazim in aqueous solutions, Water Research 34 (2000) 2951-2954.
[58] P. Mazellier, É. Leroy, B. Legube, Photochemical behavior of the fungicide carbendazim in dilute aqueous solution, Journal of Photochemistry and Photobiology A: Chemistry 153 (2002) 221-227.
[59] Y. Souissi, S. Bouchonnet, S. Bourcier, K.O. Kusk, M. Sablier, H.R. Andersen, Identification and ecotoxicity of degradation products of chloroacetamide herbicides from UV-treatment of water, Science of The Total Environment 458-460 (2013) 527-534.

865 [60] H.-J. Choi, D. Kim, T.-J. Lee, Photochemical degradation of atrazine in UV and UV/H2O2
866 process: pathways and toxic effects of products, Journal of Environmental Science and Health,
867 Part B 48 (2013) 927-934.
868 [61] B.A. Wols, D.J.H. Harmsen, E.F. Beerendonk, C.H.M. Hofman-Caris, Predicting
869 pharmaceutical degradation by UV (LP)/H2O2 processes: A kinetic model, Chemical Engineering
870 Journal 255 (2014) 334-343.
871 [62] J.H. Baxendale, J.A. Wilson, The photolysis of hydrogen peroxide at high light intensities,
872 Transactions of the Faraday Society 53 (1957) 344-356.
873 [63] S. Giannakis, S. Rtimi, C. Pulgarin, Light-Assisted Advanced Oxidation Processes for the
874 Elimination of Chemical and Microbiological Pollution of Wastewaters in Developed and
875 Developing Countries, Molecules 22 (2017) 1070.
876 [64] T. Løgager, K. Sehested, J. Holcman, Rate constants of the equilibrium reactions SO÷4 +
877 HNO3 ⇄ HSO-4 + NO˙3 and SO÷4 + NO-3 ⇄ SO2-4 + NO˙3, Radiation Physics and Chemistry 41
878 (1993) 539-543.
879 [65] M. Kwon, S. Kim, Y. Yoon, Y. Jung, T.-M. Hwang, J. Lee, J.-W. Kang, Comparative evaluation
880 of ibuprofen removal by UV/H2O2 and UV/S2O82− processes for wastewater treatment,
881 Chemical Engineering Journal 269 (2015) 379-390.
882 [66] G.P. Anipsitakis, D.D. Dionysiou, Transition metal/UV-based advanced oxidation
883 technologies for water decontamination, Applied Catalysis B: Environmental 54 (2004) 155-163.
884 [67] Y. Xiao, L. Zhang, W. Zhang, K.-Y. Lim, R.D. Webster, T.-T. Lim, Comparative evaluation of
885 iodoacids removal by UV/persulfate and UV/H2O2 processes, Water Research 102 (2016) 629-
886 639.
887 [68] J. Deng, Y. Shao, N. Gao, S. Xia, C. Tan, S. Zhou, X. Hu, Degradation of the antiepileptic drug
888 carbamazepine upon different UV-based advanced oxidation processes in water, Chemical
889 Engineering Journal 222 (2013) 150-158.
890 [69] O. Legrini, E. Oliveros, A.M. Braun, Photochemical processes for water treatment, Chemical
891 Reviews 93 (1993) 671-698.
892 [70] L. Zhou, M. Sleiman, C. Ferronato, J.-M. Chovelon, C. Richard, Reactivity of sulfate radicals
893 with natural organic matters, Environmental Chemistry Letters 15 (2017) 733-737.
894 [71] S. Miralles-Cuevas, D. Darowna, A. Wanag, S. Mozia, S. Malato, I. Oller, Comparison of
895 UV/H2O2, UV/S2O82−, solar/Fe(II)/H2O2 and solar/Fe(II)/S2O82− at pilot plant scale for the
896 elimination of micro-contaminants in natural water: An economic assessment, Chemical
897 Engineering Journal 310 (2017) 514-524.
898 [72] H.V. Lutze, S. Bircher, I. Rapp, N. Kerlin, R. Bakkour, M. Geisler, C. von Sonntag, T.C. Schmidt,
899 Degradation of Chlorotriazine Pesticides by Sulfate Radicals and the Influence of Organic Matter,
900 Environmental Science & Technology 49 (2015) 1673-1680.
901 [73] A. Adachi, T. Okano, Generation of Cyanide Ion by the Reaction of Hexamine and Losartan
902 Potassium with Sodium Hypochlorite, Journal of Health Science 54 (2008) 581-583.
903 [74] M. Isidori, M. Bellotta, M. Cangiano, A. Parrella, Estrogenic activity of pharmaceuticals in
904 the aquatic environment, Environment International 35 (2009) 826-829.
905 [75] H. Olvera-Vargas, N. Oturan, D. Buisson, E.D. van Hullebusch, M.A. Oturan, Electro-
906 Oxidation of the Pharmaceutical Furosemide: Kinetics, Mechanism, and By-Products, CLEAN –
907 Soil, Air, Water 43 (2015) 1455-1463.
908 [76] N.S. Kudryasheva, T.V. Rozhko, Effect of low-dose ionizing radiation on luminous marine
909 bacteria: radiation hormesis and toxicity, Journal of Environmental Radioactivity 142 (2015) 68-
910 77.
911 [77] V.L.K. Jennings, M.H. Rayner-Brandes, D.J. Bird, Assessing chemical toxicity with the
912 bioluminescent photobacterium (vibrio fischeri): a comparison of three commercial systems,
913 Water Research 35 (2001) 3448-3456.
914 [78] S. Rodriguez, A. Santos, A. Romero, Oxidation of priority and emerging pollutants with
915 persulfate activated by iron: Effect of iron valence and particle size, Chemical Engineering
916 Journal 318 (2017) 197-205.

[79] A.G. Trovó, T.F.S. Silva, O. Gomes, A.E.H. Machado, W.B. Neto, P.S. Muller, D. Daniel, Degradation of caffeine by photo-Fenton process: Optimization of treatment conditions using experimental design, Chemosphere 90 (2013) 170-175.
[80] E.P. da Costa, S.E.C. Bottrel, M.C.V.M. Starling, M.M.D. Leão, C.C. Amorim, Degradation of carbendazim in water via photo-Fenton in Raceway Pond Reactor: assessment of acute toxicity and transformation products, Environmental Science and Pollution Research (2018).
[81] C. Tan, N. Gao, Y. Deng, Y. Zhang, M. Sui, J. Deng, S. Zhou, Degradation of antipyrine by UV, UV/H2O2 and UV/PS, Journal of Hazardous Materials 260 (2013) 1008-1016.
[82] C. Richard, G. Guyot, A. Rivaton, O. Trubetskaya, O. Trubetskoj, L. Cavani, C. Ciavatta, Spectroscopic approach for elucidation of structural peculiarities of Andisol soil humic acid fractionated by SEC-PAGE setup, Geoderma 142 (2007) 210-216.
[83] A. Paul, R. Stösser, A. Zehl, E. Zwirnmann, R.D. Vogt, C.E.W. Steinberg, Nature and Abundance of Organic Radicals in Natural Organic Matter: Effect of pH and Irradiation, Environmental Science & Technology 40 (2006) 5897-5903.
[84] U. Kalsoom, S.S. Ashraf, M.A. Meetani, M.A. Rauf, H.N. Bhatti, Degradation and kinetics of H2O2 assisted photochemical oxidation of Remazol Turquoise Blue, Chemical Engineering Journal 200 (2012) 373-379.
[85] Y. Wang, F.A. Roddick, L. Fan, Direct and indirect photolysis of seven micropollutants in secondary effluent from a wastewater lagoon, Chemosphere 185 (2017) 297-308.
[86] Y.-H. Guan, J. Ma, D.-K. Liu, Z.-f. Ou, W. Zhang, X.-L. Gong, Q. Fu, J.C. Crittenden, Insight into chloride effect on the UV/peroxymonosulfate process, Chemical Engineering Journal 352 (2018) 477-489.
[87] R.G. Zepp, J. Hoigne, H. Bader, Nitrate-induced photooxidation of trace organic chemicals in water, Environmental Science & Technology 21 (1987) 443-450.
[88] G.-D. Fang, D.D. Dionysiou, Y. Wang, S.R. Al-Abed, D.-M. Zhou, Sulfate radical-based degradation of polychlorinated biphenyls: Effects of chloride ion and reaction kinetics, Journal of Hazardous Materials 227-228 (2012) 394-401.
[89] L. Patiny, A. Borel, ChemCalc: a building block for tomorrow's chemical infrastructure, Journal of Chemical Information and Modeling (2013).
[90] I. Dalmázio, L.S. Santos, R.P. Lopes, M.N. Eberlin, R. Augusti, Advanced Oxidation of Caffeine in Water: On-Line and Real-Time Monitoring by Electrospray Ionization Mass Spectrometry, Environmental Science & Technology 39 (2005) 5982-5988.

GRAPHICAL ABSTRACT

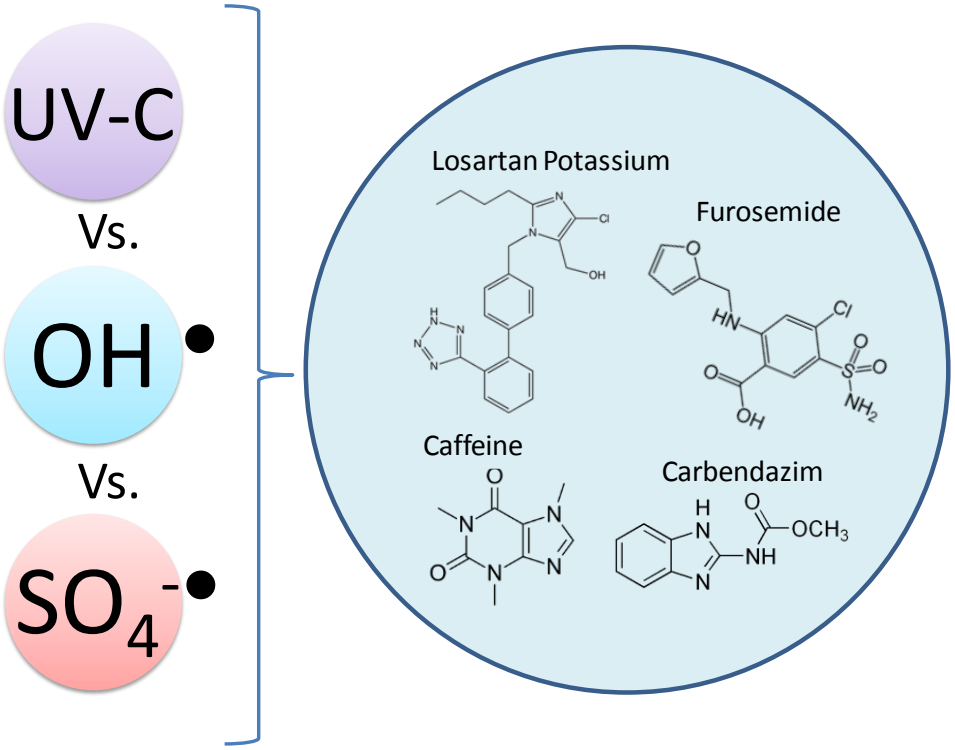

Figure 1. Photolysis (UV-C_{254nm}) of LP (2.2 µM), FRSM (3.0 µM), CAF (5.2 µM), and CBZ (5.5 µM) in ultrapure water at acidic, natural (non-adjusted), and basic pH (I_0 = 2.54 J m^{-2} s^{-1}, volume 3.5 mL) as a function of incident energy per area (mJ cm^{-2}).

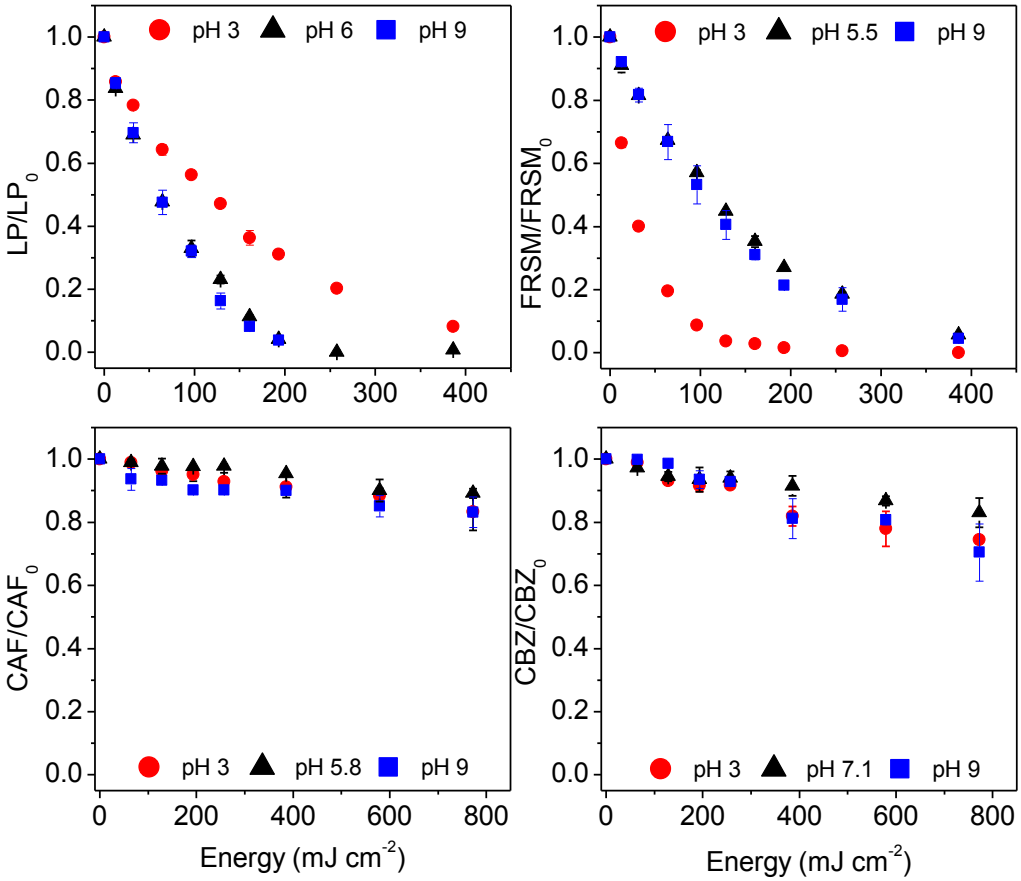

Figure 2. Left: Degradation of each target compound by UV-C AOPs: UV-C/H_2O_2 and UV-C/$S_2O_8^{2-}$. Control experiments are also presented (UV-C photolysis, H_2O_2, or $S_2O_8^{2-}$ alone). Molar ratio of H_2O_2 or $S_2O_8^{2-}$: compound = 20:1 for LP, FRSM, and CAF, and 32:1 for CBZ; I_0 = 2.41 J m^{-2} s^{-1}. Right: consumption (%) of

H_2O_2 (C_0 = 10^{-3} M), $S_2O_8^{2-}$ (C_0 = 10^{-3} M), and pH values monitored during UV-C AOPs for each of the target compounds, as functions of incident energy per unit area (mJ cm^{-2}).

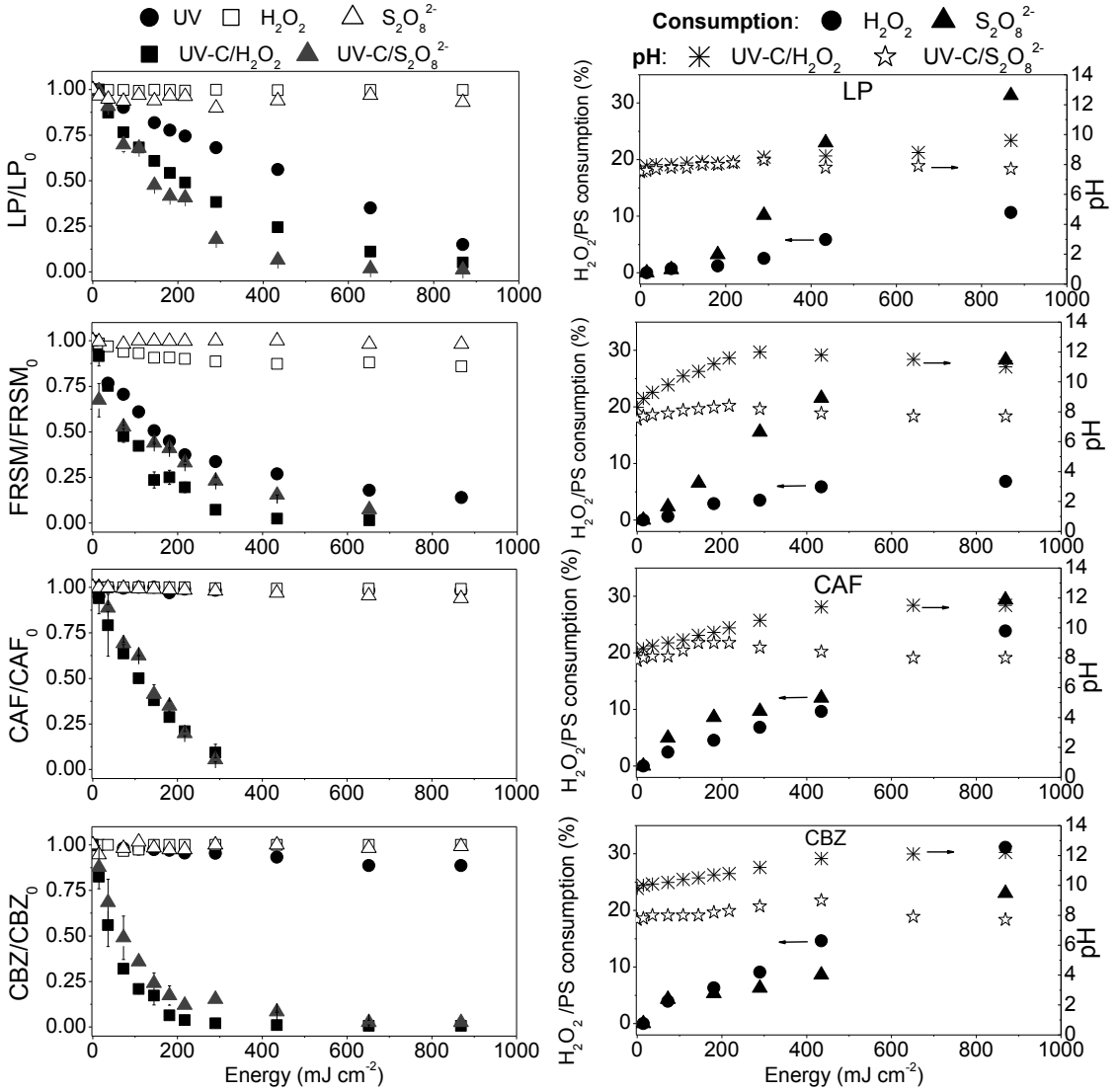

Figure 3. Acute toxicity of samples withdrawn during the degradation of target compounds via UV-C, UV-C/H_2O_2, and UV-C/$S_2O_8^{2-}$ processes, shown as functions of the total incident energy received (mJ cm^{-2}). The horizontal lines

represent the threshold of 1.21 a.T.u.; bars crossing the line thus indicate toxic samples.

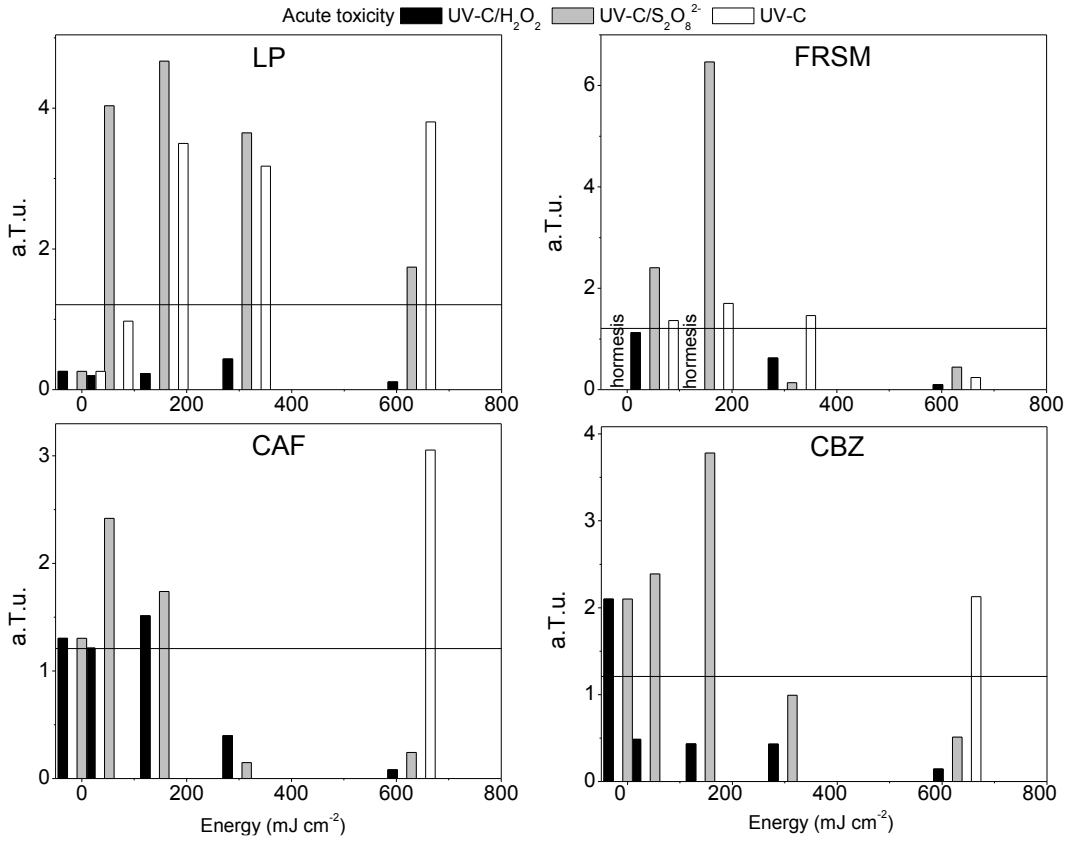

Figure 4. Degradation of LP, FRSM, CAF, and CBZ (10 µM each) in ultra-pure water and surface water by UV-C, UV-C/H_2O_2, and UV-C/$S_2O_8^{2-}$ processes ($C_{0H2O2 \text{ or } S2O82-}$ = 10^{-3} M), shown as functions of total incident energy per area (mJ

cm^{-2}).

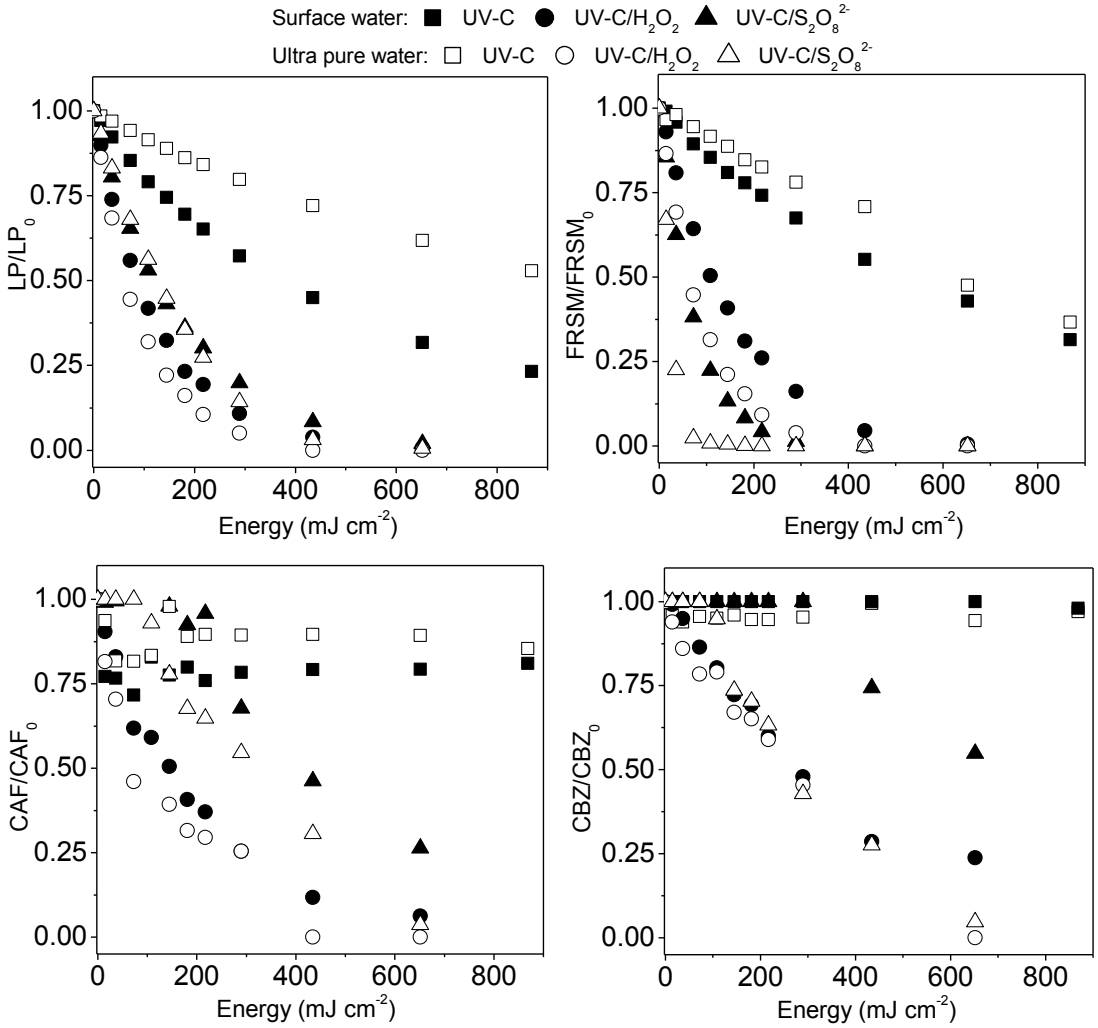

Figure 5. Reagent consumption and TOC removal during UV-C AOPs in surface water (filled symbols) and pure water (empty symbols), as functions of total incident energy per area (mJ cm^{-2}) (Initial TOC in pure water 5.4 mg L^{-1} and in surface water 6.6 mg L^{-1}).

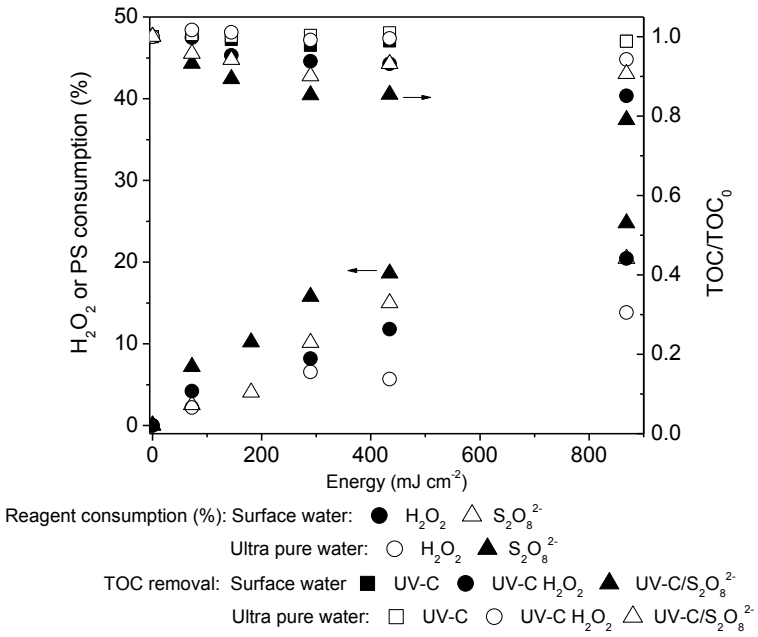

Figure 6. Mass spectra of (A) Caffeine solution in pure water, (B and D) signals corresponding to masses detected during UV-C/H_2O_2 and UV-C/$S_2O_8^{2-}$ treatments, and (C and E) mass spectra obtained after UV-C/H_2O_2 and UV-C/$S_2O_8^{2-}$ treatments with 300 mJ cm^{-2} of total incident energy.

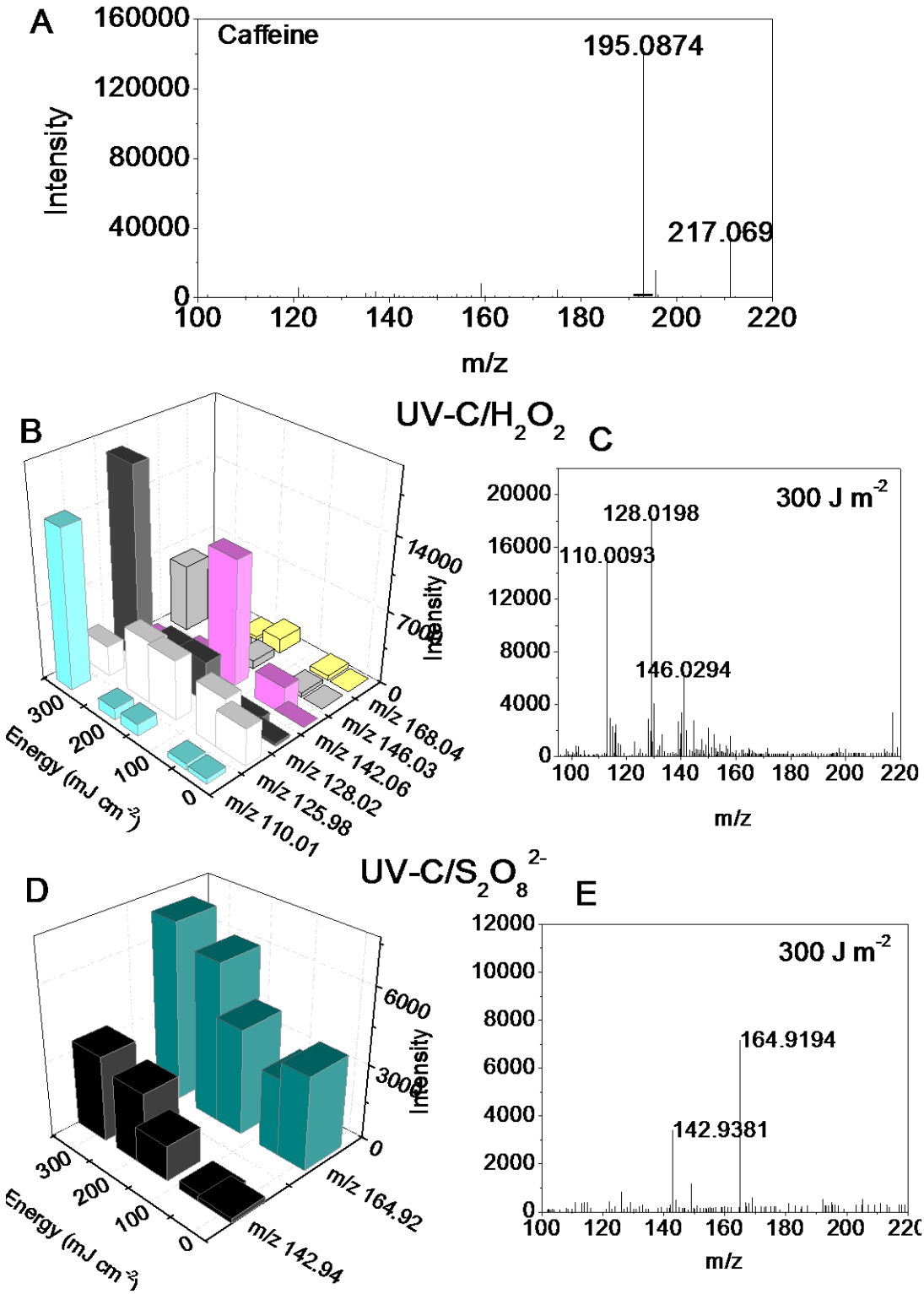

Figure 7. Degradation pathway proposed for the formation of transformation products generated during the oxidation of caffeine via UV-C/H_2O_2

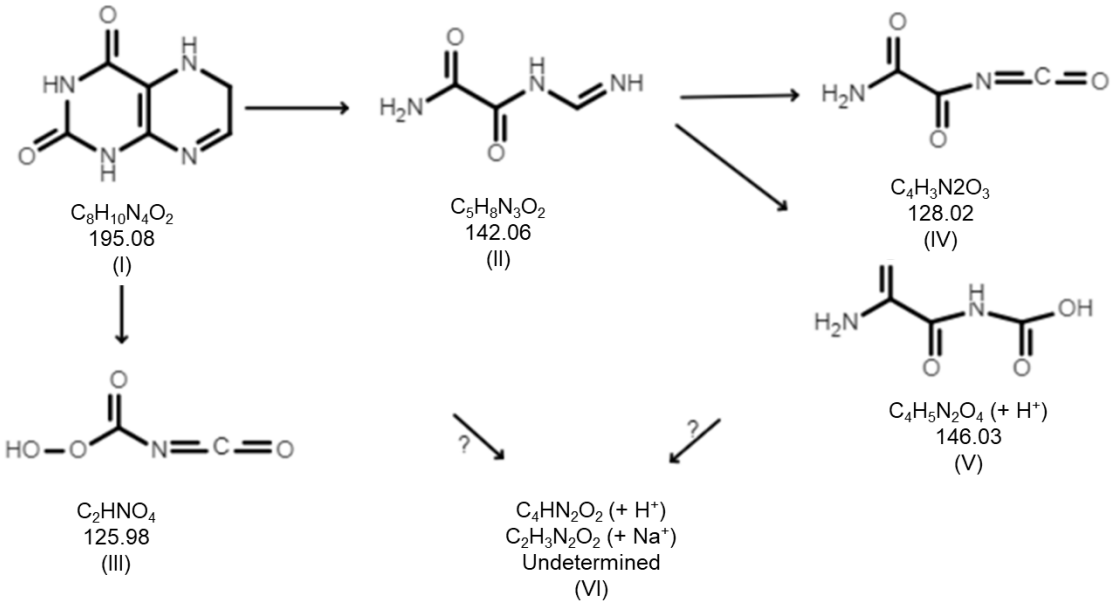

1051

1052

1053